Charge Effects on Oxygen Atom Transfer

Sean B. Seymore[1] and Seth N. Brown*

Department of Chemistry and Biochemistry, 251 Nieuwland Science Hall, University of Notre Dame, Notre Dame, Indiana 46556-5670

Received July 19, 1999

The rhenium(V) complex $[(HCpz_3)ReOCl_2]^+$ ($[\mathbf{1}]^+$), the tris(pyrazolyl)methane analogue of the known tris(pyrazolyl)borate complex $(HBpz_3)ReOCl_2$ (**2**), has been prepared. The two complexes are strikingly similar, as are the phosphine oxide adducts $[(HCpz_3)ReCl_2(OPPh_3)]Cl$ ([**3**]Cl) and $(HBpz_3)ReCl_2(OPPh_3)$ (**4**), which have been characterized by X-ray crystallography. Comparison of the bimolecular reduction of $[\mathbf{1}]BF_4$ and **2** by triarylphosphines reveals a pronounced charge effect, with the cationic species being reduced by PPh_3 about 1000 times faster than its neutral analogue in CH_2Cl_2 at room temperature. Ligand substitution of the adducts $[\mathbf{3}]^+$ and **4** is dissociative, with the cationic complex dissociating phosphine oxide about 56 times more slowly than the neutral compound. The relative impact of charge on ground and transition states in atom transfer reactions is discussed.

Introduction

There is considerable interest in the chemistry of inorganic compounds containing an oxygen atom that is multiply bonded to a transition metal in a high oxidation state. The salient feature of these compounds is their redox properties: such compounds can transfer an oxygen atom to reductants such as phosphines, sulfides, and alkenes.[2] Oxygen atom transfer chemistry has been implicated in various reactions of industrial and biological importance, including olefin epoxidation[3] and catalysis by cytochrome P-450.[4]

There is a clear need to establish the factors which control the reactivity of the metal−oxo moiety. The effects of ancillary ligands and metal oxidation state have received the most attention.[5] The effect of overall charge on metal-mediated oxygen atom transfer, in contrast, has not been explored systematically. We chose to try to isolate the effects of charge in a simple model system involving the reduction of rhenium(V) by triarylphosphines. Rhenium(V) forms a large number of stable octahedral complexes with multiple bonds to oxygen.[6] Triphenylphosphine is widely used to study oxygen atom transfer because the reactions proceed cleanly and rapidly.[5,7] Phosphine oxidation has been used to study the redox behavior of molybdenum-containing enzymes,[8] models of tungsten enzymes,[9] and oxometal porphyrin models of cytochrome P-450.[10]

Here we describe the preparation of the cationic tris(pyrazolyl)methane complex $[(HCpz_3)ReOCl_2]^+$, which differs from the known[11−13] tris(pyrazolyl)borate complex $(HBpz_3)ReOCl_2$ only in the substitution of carbon for boron and in the corresponding overall charge. It was anticipated that this change remote from the coordination sphere would only minimally perturb other steric and electronic features of the complexes. The results of a detailed kinetic study of the reduction of the two complexes by PPh_3, as well as the subsequent dissociation of $OPPh_3$ from the reduced species, thus speak directly to the differences in reactivity engendered by the change in overall charge.

Experimental Section

General Methods. Unless otherwise noted, all procedures were carried out on the benchtop. When necessary, acetonitrile, chloroform, and methylene chloride were dried over 4 Å molecular sieves, followed by CaH_2. Pyridine was dried over CaH_2. Anhydrous 1,2-dichlorobenzene (99%) was obtained from Aldrich and used without further purification. Dry ether was vacuum transferred from sodium benzophenone ketyl. $HCpz_3$,[14] $(HBpz_3)ReOCl_2$ (**2**),[13] and $ReOCl_3(OPPh_3)(SMe_2)$[15] were prepared using literature procedures. All other reagents were commercially available and used without further purification.

NMR spectra were measured on a General Electric GN-300 or a Varian-300 FT-NMR spectrometer. Chemical shifts for ^1H and $^{13}C\{^1H\}$ spectra are reported in parts per million referenced to TMS; those for ^{31}P spectra are reported in parts per million referenced to external H_3PO_4. The peaks due to the pyrazole protons are listed only as their chemical shifts and multiplicities; their coupling constants are always 2 Hz. Pyrazole H-4 protons appear as triplets, and pyrazole H-3 and H-5 protons appear as doublets. Infrared spectra were recorded

(1) Arthur J. Schmitt Presidential Fellow (1996−2000).
(2) Nugent, W. A.; Mayer, J. M. *Metal−Ligand Multiple Bonds;* Wiley: New York, 1988.
(3) Wiberg, K. B., Ed. *Oxidation in Organic Chemistry;* Academic Press: New York, 1985.
(4) Ortiz de Montellano, P. R. *Cytochrome P-450: Structure, Mechanism, and Biochemistry*; Plenum: New York, 1995.
(5) Holm, R. H. *Chem. Rev.* **1987**, *87*, 1401−1449.
(6) Rouschias, G. *Chem. Rev.* **1974**, *74*, 531−566.
(7) Moyer, B. A.; Sipe, B. K.; Meyer, T. J. *Inorg. Chem.* **1981**, *20*, 1475−1480.
(8) (a) Spiro, T. G., Ed. *Molybdenum Enzymes*; Wiley: New York, 1985. (b) Hille, R. *Chem. Rev.* **1996**, *96*, 2757−2816. (c) Holm, R. H.; Kennepohl, P.; Solomon, E. I. *Chem. Rev.* **1996**, *96*, 2239−2314.
(9) Tucci, G. C.; Donahue, J. P.; Holm, R. H. *Inorg. Chem.* **1998**, *37*, 1602−1608.
(10) (a) Bortolini, O.; Meunier, B. *J. Chem. Soc., Chem. Commun.* **1983**, 1364−1366. (b) Chin, D.-H.; LaMar, G. N.; Balch, A. L. *J. Am. Chem. Soc.* **1980**, *102*, 5945−5947. (c) Ledon, H.; Bonnet, M.; Lallemand, J.-Y. *J. Chem. Soc., Chem. Commun.* **1979**, 702−704.
(11) Abrams, M. J.; Davison, A. *Inorg. Chim. Acta* **1984**, *82*, 125−128.
(12) Degnan, I. A.; Behm, J.; Cook, M. R.; Herrmann, W. A. *Inorg. Chem.* **1991**, *30*, 2165−2170.
(13) Brown, S. N.; Mayer, J. M. *Inorg. Chem.* **1992**, *31*, 4091−4100.
(14) Julia, S.; del Mazo, J. M.; Avila, L.; Elguero, J. *Org. Prep. Proc. Int.* **1984**, *16*, 299−307.
(15) Grove, D. E.; Wilkinson, G. *J. Chem. Soc. A* **1966**, 1224−1230.

10.1021/ic990851b CCC: $19.00
Published on Web 12/28/1999

as evaporated films on KBr plates on a Perkin-Elmer Paragon 1000 FT-IR spectrometer. UV−vis data were collected on a Beckman DU-7500 diode-array spectrophotometer equipped with a multicell transport block. Mass spectra were obtained on a JEOL JMS-AX 505HA mass spectrometer using the FAB ionization mode and 3-nitrobenzyl alcohol as a matrix. In all cases, observed intensities were in satisfactory agreement with calculated isotopic distributions. Elemental analyses were performed by M-H-W Laboratories (Phoenix, AZ).

[(HCpz$_3$)ReOCl$_2$]Cl ([1]Cl). To a 50 mL round-bottom flask were added a magnetic stirbar, ReOCl$_3$(OPPh$_3$)(SMe$_2$) (1.28 g, 1.97 mmol), and HCpz$_3$ (0.44 g, 2.04 mmol). A Teflon needle valve was attached to the flask, which was then affixed to a vacuum line. Dry CH_2Cl_2 (20 mL) was added by vacuum transfer, and the solution was stirred for 4.5 h. After the volume was reduced by 50%, ether (10 mL) was condensed on top of the blue solution. The next day, the flask was removed from the vacuum line and the blue solid collected on a glass frit, washed with ether, and air-dried to yield 0.94 g of [**1**]Cl (91%). ^{1}H NMR ($CDCl_3$): δ 6.24 (t, 1H, pz trans to oxo); 6.92 (t, 2H, pz cis to oxo); 7.56 (d, 1H, pz trans to oxo); 8.42 (d, 2H, pz cis to oxo); 8.66 (d, 1H, pz trans to oxo); 9.32 (d, 2H, pz cis to oxo); 12.54 (s, 1H, pz$_3$C*H*). ^{13}C{^{1}H} NMR ($CDCl_3$): δ 150.8, 148.8, 141.0, 135.2, 111.3, 108.8, 75.3. IR (cm^{-1}): 1504 (m), 1444 (m), 1410 (w), 1390 (m), 1271 (s), 1244 (s), 1094 (m), 1062 (s), 1007 (s), 986 (s, Re═O), 908 (m), 854 (m), 830 (w), 765 (s). UV−Vis (CH_2Cl_2): λ_{max} = 678 nm, ϵ = 120 M^{-1} cm^{-1}. FABMS: *m*/*z* 487 (M$^+$). Anal. Calcd for $C_{10}H_{10}N_6OCl_3Re$: C, 22.97; H, 1.93; N, 16.08. Found: C, 22.80; H, 1.79; N, 15.83.

[(HCpz$_3$)ReOCl$_2$]BF$_4$ ([1]BF$_4$). To a 50 mL Erlenmeyer flask were added [**1**]Cl (478 mg, 0.91 mmol), $AgBF_4$ (Aldrich, 178 mg, 0.91 mmol), CH_3CN (20 mL), and a magnetic stirbar. After the mixture was stirred for 30 min, the white solid was removed by suction filtration, and the volume of the dark blue solution reduced to 10 mL on the rotary evaporator. Vapor diffusion of ether (∼10 mL) into the solution resulted in the precipitation of more white solid. The insoluble material was removed by suction filtration, and the blue solution evaporated to dryness. The blue residue was crystallized from acetonitrile/ether to furnish 301 mg of analytically pure [**1**]BF$_4$ (56%). ^{1}H NMR (CD_3CN): δ 6.31 (t, 1H, pz trans to oxo); 6.97 (t, 2H, pz cis to oxo); 7.57 (d, 1H, pz trans to oxo); 8.09 (d, 1H, pz trans to oxo); 8.48 (d, 2H, pz cis to oxo); 8.62 (d, 2H, pz cis to oxo); 9.19 (s, 1H, pz$_3$C*H*). IR (cm^{-1}): 1508 (m), 1448 (w), 1409 (m), 1393 (m), 1264 (m), 1248 (m), 1224 (w), 1065 (vs, br, BF$_4^-$), 987 (s, Re═O), 908 (s), 854 (m), 773 (s). Anal. Calcd for $C_{10}H_{10}N_6BOCl_2F_4Re$: C, 20.92; H, 1.76; N, 14.64. Found: C, 21.04; H, 1.61; N, 14.56.

[(HCpz$_3$)ReCl$_2$(OPPh$_3$)]Cl ([3]Cl). To a 25 mL Erlenmeyer flask were added [**1**]Cl (59 mg, 0.11 mmol), PPh_3 (102 mg, 0.39 mmol), and CH_3CN (10 mL). After the mixture was stirred for 1 h, the crude brown product was collected by filtration and washed with two 10 mL aliquots of ether. More product was precipitated by adding ether to the mother liquor. The combined brown solids were recrystallized from chloroform/ether. The yellow crystals were collected by suction filtration, washed with ether, and air-dried. The total yield of [**3**]Cl was 33 mg (37%). ^{1}H NMR ($CDCl_3$): δ −20.85 (d, 1H, pz trans to OPPh$_3$); −17.14 (d, 2H, pz cis to OPPh$_3$); −15.91 (d, 1H, pz trans to OPPh$_3$); −9.36 (d, 2H, pz cis to OPPh$_3$); 4.35 (s, 1H, pz$_3$C*H*); 7.15 (dd, *J* = 13, 8 Hz, 6H, ortho); 7.56 (t, *J* = 7 Hz, 3H, para); 7.70 (td, *J* = 8, 3 Hz, 6H, meta); 8.98 (t, 1H, pz trans to OPPh$_3$); 9.02 (t, 2H, pz cis to OPPh$_3$). ^{31}P{^{1}H} NMR (CD_2Cl_2): δ 170.34. IR (cm^{-1}): 1440 (m), 1404 (s), 1276 (s), 1243 (w), 1122 (s, P−O), 855 (m), 778 (s). FABMS: *m*/*z* 749 (M$^+$). Anal. Calcd for $C_{28}H_{25}N_6Cl_3OPRe$: C, 42.83; H, 3.22; N, 10.70. Found: C, 43.00; H, 3.10; N, 11.00.

[(HCpz$_3$)ReCl$_2$(OPPh$_3$)]BF$_4$ ([3]BF$_4$). To a 25 mL Erlenmeyer flask were added [**1**]BF$_4$ (301 mg, 0.53 mmol), PPh_3 (1.40 g, 5.33 mmol), and CH_3CN (15 mL). After being stirred for 10 min, the yellow solution was evaporated. The residual solid was washed with ether, and two crops of crystals were grown from CH_3CN/ether. The yellow crystals were collected by suction filtration, washed with ether, and air-dried. Yield: 290 mg (51%). ^{1}H NMR (CD_2Cl_2): δ −21.25 (d, 1H, pz trans to OPPh$_3$); −17.72 (d, 2H, pz cis to OPPh$_3$); −16.18 (d, 1H, pz trans to OPPh$_3$); −9.71 (d, 2H, pz cis to OPPh$_3$); 1.62 (s, 1H, pz$_3$C*H*); 7.28 (dd, *J* = 13, 8 Hz, 6H, ortho); 7.60 (t, *J* = 7 Hz, 3H, para); 7.73 (td, *J* = 8, 3 Hz, 6H, meta); 9.28 (t, 1H, pz trans to OPPh$_3$); 9.37 (t, 2H, pz cis to OPPh$_3$). IR (cm^{-1}): 1438 (m), 1404 (m), 1270 (w), 1241 (w), 1141 (s), 1123 (s, P−O), 1054 (vs, br, BF$_4^-$), 854 (w), 773 (w). UV−vis (CH_2Cl_2): λ_{max} = 370 nm, ϵ = 3.6 × 10^3 M^{-1} cm^{-1}. Anal. Calcd for $C_{28}H_{25}N_6BOCl_2F_4PRe$: C, 40.21; H, 3.02; N, 10.05. Found: C, 40.40; H, 3.16; N, 10.15.

(HBpz$_3$)ReCl$_2$(OPPh$_3$) (4). Into a 50 mL Erlenmeyer flask were placed (HBpz$_3$)ReOCl$_2$ (**2**, 330 mg, 0.68 mmol), PPh_3 (3.51 g, 13.37 mmol), and CH_2Cl_2 (8.5 mL). After being stirred for 24 h, the solution was evaporated to dryness, and the solid residue washed with ether (100 mL). The crude material was recrystallized from CH_2Cl_2/ether to yield orange crystals of the product. Yield: 308 mg (61%). ^{1}H NMR ($CDCl_3$): δ −19.11 (d, 1H, pz trans to OPPh$_3$); −14.76 (d, 2H, pz cis to OPPh$_3$); −13.12 (d, 1H, pz trans to OPPh$_3$); −5.38 (d, 2H, pz cis to OPPh$_3$); −3.40 (s, 1H, pz$_3$B*H*); 6.09 (t, 1H, pz trans to OPPh$_3$); 6.76 (dd, *J* = 13, 8 Hz, 6H, ortho); 7.05 (t, 2H, pz cis to OPPh$_3$); 7.45 (t, *J* = 7 Hz, 3H, para); 7.62 (td, *J* = 8, 3 Hz, 6H, meta). ^{31}P{^{1}H} NMR (CD_2Cl_2): δ 120.48. IR (cm^{-1}): 1636 (w), 1590 (m), 1496 (m), 1486 (m), 1438 (s), 1403 (s), 1388 (m), 1305 (s), 1266 (m), 1207 (s), 1155 (vs, P−O), 1119 (s), 1092 (m), 1072 (m), 1047 (s), 1028 (m), 998 (m), 919 (w), 885 (w), 851 (w), 812 (w), 787 (s). UV−vis (CH_2Cl_2): λ_{max} = 338 nm, ϵ = 3.6 × 10^3 M^{-1} cm^{-1}. FABMS: *m*/*z* 748 (M$^+$). Anal. Calcd for $C_{27}H_{25}N_6BOCl_2PRe$: C, 43.33; H, 3.37; N, 11.23. Found: C, 43.72; H, 3.61; N, 11.33.

[(HCpz$_3$)Re(py)Cl$_2$]Cl was prepared on a small scale by adding [**3**]Cl (1.90 mg, 2.40 μmol), dry pyridine (1.0 μL, 12.4 μmol), and dry CD_2Cl_2 (1 mL) to a valved NMR tube in the drybox. The tube was heated at 50 °C for two weeks; NMR monitoring of the yellow solution showed the presence of starting material throughout this period. The tube was subsequently heated in a 70 °C oil bath until the reaction was complete (118 h). ^{1}H NMR (CD_2Cl_2): δ −18.22 (d, 2H, pz cis to py); −14.14 (d, 2H, pz cis to py); −12.81 (d, 1H, pz cis to py); −8.94 (d, *J* = 5 Hz, 2H, py 2,6-H); −3.94 (t, *J* = 8 Hz, 1H, py 4-H); −1.32 (d, 1H, pz trans to py); 5.38 (s, 1H, pz$_3$C*H*); 7.41 (t, 2H, pz cis to py); 13.03 (t, 1H, pz trans to py); 17.25 (t, *J* = 7 Hz, 2H, py 3,5-H). UV−vis (1,2-$C_6H_4Cl_2$): λ_{max} = 432 nm, ϵ = 1.5 × 10^3 M^{-1} cm^{-1}. FABMS: *m*/*z* 550 (M$^+$).

[{(η^2-HCpz$_3$)ReOCl$_2$}$_2$(μ-Cl)][ReOCl$_4$] was generated in solution by dissolving [**1**]Cl (3.00 mg, 5.70 μmol) in CD_3CN (1 mL). The suspension was filtered and the filtrate added to a NMR tube. The blue solution was monitored by ^{1}H NMR for one week. The resulting equilibrium mixture included the starting material, free HCpz$_3$, and the new product. ^{1}H NMR (CD_3CN): δ 6.38 (t, 1H); 6.66 (d, 1H); 7.12 (t, 2H); 7.63 (d, 1H); 8.76 (d, 2H); 9.16 (s, 1H; pz$_3$C*H*); 9.23 (d, 2H). FABMS: *m*/*z* 1009 (M$^+$).

X-ray Structure Determinations of [(HCpz$_3$)Re(OPPh$_3$)Cl$_2$]Cl·0.5 CDCl$_3$ ([3]Cl·0.5 CDCl$_3$) and (HBpz$_3$)Re(OPPh$_3$)Cl$_2$·C$_6$H$_6$ (4·C$_6$H$_6$). Orange plates of the salt [**3**]Cl were deposited after slow diffusion of ether into a solution of the complex in $CDCl_3$. A crystal was glued to the tip of a glass fiber in the air and examined on an Enraf-Nonius CAD4 diffractometer using Mo Kα radiation with a graphite monochromator (λ = 0.710 73 Å). The crystal was triclinic (space group $P\bar{1}$). The unit cell was determined on the basis of 24 reflections with 15.0° < θ < 15.9°. Crystal quality was monitored by recording three standard reflections approximately every 180 reflections measured; decay was negligible. An empirical absorption correction was applied (μ = 4.336 mm^{-1}, transmission factors 0.8166−0.9999). The rhenium atom was located on a Patterson map, the remaining non-hydrogen atoms were found on difference Fourier syntheses, and hydrogens were placed in calculated positions. Two additional peaks were found on the difference map; these were assigned to the C and a Cl of a disordered chloroform molecule located on the inversion center. There were additional small peaks near these on the difference map, but the other two Cl atoms could not be refined successfully and were omitted from the final model. Final full-matrix least-squares refinement on F^2 converged at R = 0.0301 for 5166 reflections with $F_o > 4\sigma(F_o)$ and R = 0.0330 for all data (wR2 = 0.0830 and 0.0866, respectively).

All calculations used SHELXTL (Bruker Analytical X-ray Systems), with scattering factors and anomalous dispersion terms taken from the literature.[16]

Yellow prisms of the tris(pyrazolyl)borate complex **4** were deposited after slow diffusion of benzene into a solution of the complex in 1,2-dichloroethane. A crystal was glued to the tip of a glass fiber in the air and examined as described above. The unit cell (triclinic, $P\bar{1}$) was determined on the basis of 24 reflections with $14.7° < \theta < 16.0°$. Decay was negligible, and an empirical absorption correction was applied ($\mu = 3.872$ mm^{-1}, transmission factors 0.2240−0.3078). Data reduction and analysis were as described above except for the treatment of the hydrogen atoms, which were found on difference Fourier maps and refined isotropically, except those on the solvent molecule, which were placed in calculated positions. Final full-matrix least-squares refinement on F^2 converged at $R = 0.0180$ for 5605 reflections with $F_o > 4\sigma(F_o)$ and $R = 0.0197$ for all data (wR2 = 0.0452 and 0.0462, respectively).

Kinetics. UV−vis data were collected on a Beckman DU-7500 diode-array spectrophotometer equipped with a multicell transport block. The temperature was regulated by a circulating water/ethylene glycol mixture and was measured by a thermocouple inserted in the cell block. Solutions were prepared in 1 cm quartz cells fitted with septum caps.

The order of the phosphine oxidation process was determined in dichloromethane at room temperature. For [**1**]Cl, the reaction was followed by measuring the decrease in absorbance of the starting material at 678 nm. Eight experiments were done under pseudo-first-order conditions with initial Re(V) concentrations ranging from 8.1×10^{-4} to 1.9×10^{-3} M, and with excess phosphine (10−80 equiv). For each experimental run, three cuvettes were prepared. A similar procedure was followed for **2**, measuring the absorbance at 690 nm, and using initial Re(V) concentrations from 4.4×10^{-3} to 8.3×10^{-3} M with 40−80 equiv of phosphine.

The ligand substitution process was studied using the phosphine oxide adducts ([**3**]BF_4 and **4**) and excess pyridine. The reactions were monitored by following the appearance of the pyridine adducts ($\lambda_{max} = 432$ nm for [**3**]BF_4; $\lambda_{max} = 469$ nm for **4**). The dependence of the rate of ligand substitution on pyridine concentration was determined at experimentally convenient temperatures (73 and 47 °C, respectively), with [Re(III)] = $(1.2-3.9) \times 10^{-4}$ M and $[py]_0 = 4.1 \times 10^{-2}$ to 4.1×10^{-1} M.

Pseudo-first-order rate constants were obtained by using a least-squares fit to the equation $\ln|A_\infty - A| = -kt + \ln|A_\infty - A_0|$. These plots were linear for at least 4 half-lives. Activation parameters were determined from plots of $\ln(k/T)$ vs $1/T$.[17]

Reversibility Experiment. Into an NMR tube sealed to a ground-glass joint were added [**3**]Cl (3.9 mg, 5.0 μmol) and $P(C_6D_5)_3$ (29.4 mg, 0.11 mmol). Into another tube were added **4** (10.0 mg, 13.4 μmol) and $P(C_6D_5)_3$ (42.1 mg, 0.15 mmol). After evacuation on the vacuum line, approximately 1 mL of dry CD_2Cl_2 was transferred to each tube at −78 °C. The tubes were flame-sealed under vacuum and subsequently monitored by ^{1}H and ^{31}P NMR spectroscopy. The tubes were heated by full immersion in an 85 °C water bath. Reaction progress was monitored by observing the disappearance of the starting material.

Photochemistry. In the drybox **4** (2.6 mg, 3.8 μmol) and dimethyl terephthalate (0.1 mg, used as an internal standard) were dissolved in 2 mL of dry CD_3CN. A syringe was used to transfer 1 mL of the yellow solution to each of two NMR tubes, which were capped and removed from the drybox. One tube was wrapped securely in aluminum foil. The tubes were irradiated for 4 h in a Rayonet photochemical reactor equipped with 350 nm Ne bulbs. ^{1}H NMR spectra were obtained at various intervals throughout the irradiation process. The reaction progress was monitored by observing the appearance of the $Re^{III}-NCCD_3$ adduct.

Results

Synthesis and Characterization of Tris(pyrazolyl)methane Rhenium Complexes. In our efforts to prepare an isoelectronic and isostructural analogue to the known tris(pyrazolyl)borate complex $(HBpz_3)ReOCl_2$ (**2**),[11−13] we set out to isolate salts of the hitherto unknown tris(pyrazolyl)methane complex $[(HCpz_3)ReOCl_2]^+$ ($[\mathbf{1}]^+$). While the rhenium(VII) complex $[(HCpz_3)ReO_3]ReO_4$ has been isolated,[18] no other high-valent rhenium tris(pyrazolyl)methane complexes have been reported. This contrasts with the rich chemistry of rhenium(V) and rhenium(III) involving tris[19] and tetrakis[20] pyrazolylborate ligands.

Stirring $ReOCl_3(OPPh_3)(SMe_2)$[15,21] in dichloromethane with $HCpz_3$[14,22] for 4.5 h yields a blue solution; addition of ether precipitates the air stable salt [**1**]Cl (eq 1). [**1**]Cl is sparingly

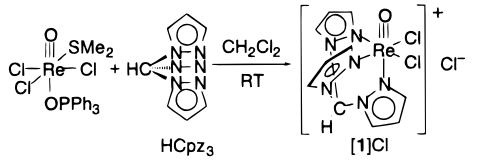

(1)

soluble in polar organic solvents such as CH_2Cl_2, $CHCl_3$, and CH_3CN, and insoluble in ether, benzene, alcohols, and water. Its ^{1}H NMR spectrum indicates that the complex has mirror symmetry, consistent with tridentate coordination of the $HCpz_3$ ligand. FAB mass spectrometry confirms the composition of the cation, and a strong stretch in the IR at 985 cm^{-1} indicates the presence of the terminal oxo group.

Attempts to grow a crystal of [**1**]Cl suitable for X-ray diffraction structure determination were unsuccessful. A crystal of the perrhenate salt [**1**]ReO_4 was studied by X-ray diffraction, which confirmed tridentate binding of the $HCpz_3$ ligand.[23] Refinement of the structure was complicated by the presence of two independent molecules in the unit cell, and the determination of accurate metrical data was frustrated by positional disorder involving the oxo and chloride ligands.[24] A similar disorder problem is observed with crystals of $(HBpz_3)ReOCl_2$ (**2**).[25] The latter is isostructural with $(HBpz_3)MoOCl_2$, whose disorder has been described in detail in the literature.[26]

The tetrafluoroborate salt of $[\mathbf{1}]^+$ was prepared by metathesis of [**1**]Cl with $AgBF_4$ in acetonitrile. Surprisingly, the ^{1}H NMR

(16) *International Tables of Crystallography*; Kluwer Academic Publishers: Dordrecht, The Netherlands, 1992; Vol. C.
(17) Frost, A. A.; Pearson, R. G. *Kinetics and Mechanism*, 2nd ed.; Wiley: New York, 1961.
(18) Herrmann, W. A.; Roesky, P. W.; Kuhn, F. E.; Elison, M.; Artus, G.; Scherer, W.; Romao, C. C.; Lopes, A.; Basset, J. M. *Inorg. Chem.* **1995**, *34*, 4701−4707.
(19) (a) Thomas, J. A.; Davison, A. *Inorg. Chim. Acta* **1991**, *190*, 231−235. (b) Tisato, F.; Bolzati, C.; Duatti, A.: Bandoli, G.; Refosco, F. *Inorg. Chem.* **1993**, *32*, 2042−2048. (c) DuMez, D. D., Mayer, J. M. *J. Am. Chem. Soc.* **1996**, *118*, 12416−12423. (d) Masui, C. S.; Mayer, J. M. *Inorg. Chim. Acta* **1996**, *251*, 325−333. (e) Herberhold, M.; Jin, G. X.; Milius, W. *J. Organomet. Chem.* **1996**, *512*, 111−116. (f) Brown, S. N.; Myers, A. W.; Fulton, J. R.; Mayer, J. M. *Organometallics* **1998**, *17*, 3364−3374. (g) Doerrer, L. H.; Galsworthy, J. R.; Green, M. L. H.; Leech, M. A. *J. Chem. Soc., Dalton Trans.* **1998**, 2483−2487.
(20) (a) Paulo, A.; Reddy, K. R.; Domingos, A.; Santos, I. *Inorg. Chem.* **1998**, *37*, 6807−6813. (b) Paulo, A.; Domingos, A.; Santos, I. *Inorg. Chem.* **1996**, *35*, 1798−1807. (c) Paulo, A.; Domingos, A.; Marcalo, J.; Dematos, A. P.; Santos, I. *Inorg. Chem.* **1995**, *34*, 2113-2120. (d) Paulo, A.; Domingos, A.; Dematos, A. P.; Santos, I. Carvalho, M. F. N. N.; Pombeiro, A. J. L. *Inorg. Chem.* **1994**, *33*, 4729−4737.
(21) (a) Bryan, J. C.; Stenkamp, R. E.; Tulip, T. H.; Mayer, J. M. *Inorg. Chem.* **1987**, *26*, 2283−2288. (b) Abu-Omar, M. M.; Khan, S. I. *Inorg. Chem.* **1998**, *37*, 4979−4985.
(22) Jameson, D. L.; Castellano, R. K. *Inorg. Synth.* **1998**, *32*, 59−61.
(23) Crystal data for [**1**]ReO_4·1.5$CDCl_3$: $C_{11.5}H_{10}D_{1.5}Cl_{6.5}N_6O_5Re_2$, green, $M = 918.14$, $T = 293$ K, triclinic, space group $P\bar{1}$, $a = 12.028(3)$ Å, $b = 15.492(3)$ Å, $c = 16.024(4)$ Å, $\alpha = 78.52(2)°$, $\beta = 74.90(2)°$, $\gamma = 67.94(2)°$, $V = 2654.7(11)$ Å^3, $Z = 4$, $\rho_c = 2.297$ g cm^{-3}, μ(Mo Kα) = 0.979 mm^{-1}, $F(000) = 1692$, crystal size $0.35 \times 0.20 \times 0.18$ mm. A total of 9345 unique reflections with $\theta = 2.00-24.99°$ were collected. For 7179 reflections with $I > 4\sigma(I)$, $R = 0.1292$ and GOF-(F^2) = 1.078.
(24) Parkin, G. *Chem. Rev.* **1993**, *93*, 887−911.

spectrum of [**1**]BF_4 differs from that of the chloride salt in the location of the methine proton (δ 9.19 in [**1**]BF_4 vs δ 12.19 in [**1**]Cl in CD_3CN). Other spectroscopic characteristics (UV−vis, IR) are essentially unaffected by the counterion.

Solutions of [**1**]Cl are stable for weeks at room temperature in noncoordinating solvents. However, [**1**]Cl undergoes ligand substitution in acetonitrile over several days to form an equilibrium mixture of products. ^{1}H NMR and FAB mass spectrometric analyses show unreacted starting material, free $HCpz_3$, and a new species which we assign as $[\{(\eta^2\text{-}HCpz_3)\text{-}ReOCl_2\}_2(\mu\text{-}Cl)]^+$. The mass spectrum shows a prominent peak at $m/z = 1009$ which possesses an isotope pattern consistent with the presence of two rhenium and five chlorine atoms. The ^{1}H NMR shows new pyrazole triplets in a 2:1 ratio, four new doublets (2:2:1:1 ratio), and a methine C−H singlet; these all identify a species possessing mirror symmetry. The methine C−H resonances of the dimer and of free $HCpz_3$ always appear in a 2:1 ratio, which suggests that 3 equiv of [**1**]Cl is required to form 1 equiv of the dimer, consistent with the stoichiometry of eq 2. The tetrafluoroborate salt [**1**]BF_4 is stable indefinitely in CD_3CN.

$$3\ [(HCpz_3)ReOCl_2]Cl \underset{}{\overset{CD_3CN}{\rightleftharpoons}} [\{\eta^2\text{-}(HCpz_3)ReOCl_2\}_2(\mu\text{-}Cl)]^+\ ReOCl_4^-\ +\ HCpz_3 \qquad (2)$$

Synthesis and Structure of Rhenium(III) Compounds. When [**1**]Cl is stirred in the presence of PPh_3, oxygen atom transfer takes place within 1 h to produce the isolable phosphine oxide adduct $[(HCpz_3)ReCl_2(OPPh_3)]Cl$ ([**3**]Cl, eq 3). The tetrafluoroborate salt reacts analogously to give [**3**]BF_4.

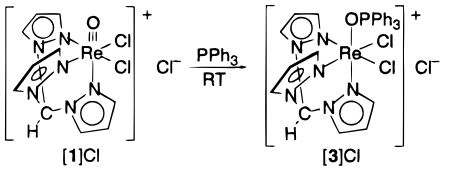

[**1**]Cl [**3**]Cl (3)

Mass spectra show the parent ion $[\mathbf{3}]^+$ at $m/z = 749$, and the presence of bound phosphine oxide is confirmed by the P−O stretch in the IR ($\nu_{PO} = 1122$ cm^{-1} for [**3**]Cl). The ^{1}H NMR spectra are paramagnetically shifted but extremely sharp, which is characteristic of octahedral Re(III) complexes.[27] The sharp spectrum allows one to observe normal H−H coupling constants, even the 2 Hz couplings characteristic of the pyrazole protons. Resonances for the ortho and meta hydrogens show coupling to phosphorus, which suggests that the ^{31}P nucleus relaxes rather slowly. This was confirmed by the observation of a sharp ^{31}P-$\{^1$H$\}$ resonance at δ 170.34 in CD_2Cl_2. Observation of ^{31}P NMR spectra of paramagnets is rare but precedented.[20d,28]

The neutral tris(pyrazolyl)borate analogue of $[\mathbf{3}]^+$, $(HBpz_3)ReCl_2(OPPh_3)$ (**4**), is presumably an intermediate in reported preparations of rhenium(III) complexes $(HBpz_3)ReCl_2(L)$ from the oxo complex **2**, PPh_3, and excess ligand.[11,29] However, the phosphine oxide adduct **4** has never been isolated or observed directly because oxygen atom transfer is usually slower than subsequent displacement of the phosphine oxide ligand. We have successfully prepared **4** by using high concentrations of PPh_3 and relatively low temperatures. Under these conditions, bimolecular atom transfer is much faster than unimolecular ligand exchange (vide infra), and **4** can be isolated uncontaminated by the phosphine adduct $(HBpz_3)ReCl_2(PPh_3)$.[11]

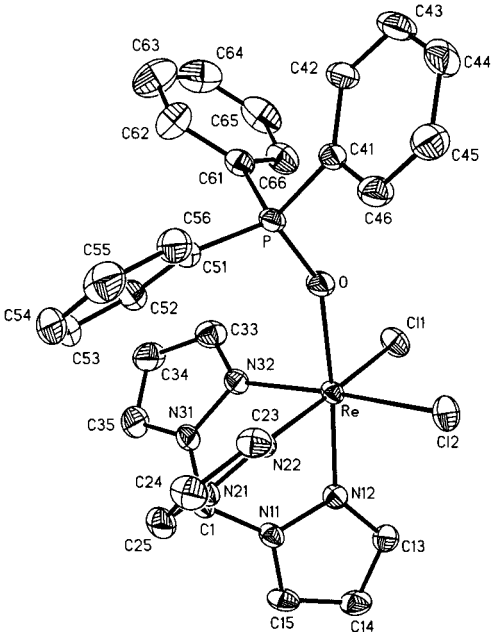

Figure 1. SHELXTL plot (30% thermal ellipsoids) of the cation of $[(HCpz_3)ReCl_2(OPPh_3)]Cl{\cdot}0.5CDCl_3$ ([**3**]Cl·0.5$CDCl_3$). Hydrogen atoms are omitted for clarity.

The structures of the tris(pyrazolyl)methane complex [**3**]Cl (Figure 1) and the tris(pyrazolyl)borate complex **4** (Figure 2) were determined by single-crystal X-ray diffraction. Crystallographic details are listed in Table 1, and bond distances and angles in Table 2. The structures are remarkably similar. The only statistically significant differences in metal−ligand distances are the Re−Cl bond lengths, which in cationic $[\mathbf{3}]^+$ are slightly shorter than in neutral **4**. The observed phosphorus−oxygen distances (1.499(4) Å av) and Re−O−P bond angles (151° av) are typical of d^4 phosphine oxide adducts.[30]

Reduction Kinetics. The kinetics of the reduction of the rhenium(V) oxo compounds [**1**]Cl, [**1**]BF_4, and **2** by triphenylphosphine were studied spectrophotometrically under pseudo-first-order conditions (excess PPh_3) at 25.3 °C in dichloromethane. The reactions obey first-order kinetics to ≥4 half-lives (Figure S1, Supporting Information), and are also observed to be first-order in triphenylphosphine. Second-order rate constants were extracted from the linear plots of k_{obs} versus $[PPh_3]$ (Figure S2); these give $k_{red} = 0.047(8)$ M^{-1} s^{-1} for

(25) Crystal data for **2**: $C_9H_{10}BCl_2N_6ORe$, blue, $M = 486.14$, $T = 293$ K, monoclinic, space group *Cc*, $a = 15.1181(21)$ Å, $b = 7.9611(15)$ Å, $c = 13.3972(23)$ Å, $\beta = 108.498(13)°$, $V = 1477.3(4)$ Å^3, $Z = 4$, $\rho_c = 2.186$ g cm^{-3}, μ(Mo Kα) = 0.859 mm^{-1}, $F(000) = 912$, crystal size 0.22 × 0.10 × 0.09 mm. A total of 2360 unique reflections with $\theta = 3.01-24.99°$ were collected. For 2235 reflections with $I > 4\sigma(I)$, $R = 0.0439$ and GOF(F^2) = 1.096.

(26) Lincoln, S.; Koch, S. A. *Inorg. Chem.* **1986**, *25*, 1594−1602.

(27) (a) Chatt, J.; Leigh, G. J.; Mingos, D. M. P. *J. Chem. Soc. A* **1969**, 1674−1680. (b) Rossi, R.; Duatti, A.; Magon, L.; Casellato, U.; Graziani, R.; Toniolo, L. *J. Chem. Soc., Dalton Trans.* **1982**, 1949−1952.

(28) Demadis, K. D.; Bakir, M.; Klesczewski, B. G.; Williams, D. S.; White, P. S.; Meyer, T. J. *Inorg. Chim. Acta* **1998**, *270*, 511−526.

(29) Brown, S. N.; Mayer, J. M. *Organometallics* **1995**, *14*, 2951−2960.

(30) (a) Christie, J. A.; Collins, T. J.; Krafft, T. E.; Santarsiero, B. D.; Spies, G. H. *J. Chem. Soc., Chem. Commun.* **1984**, 198−199. (b) Mronga, N.; Weller, F.; Dehnicke, K. *Z. Anorg. Allg. Chem.* **1983**, *502*, 35−44. (c) Philipp, G.; Wocadlo, S.; Massa, W.; Dehnicke, K.; Fenske, D.; Maichle-Mossmer, C.; Niquet, E.; Strähle, J. *Z. Naturforsch. B* **1995**, *50*, 1−10. (d) Menon, M.; Pramanik, A.; Bag, N.; Chakravorty, A. *Inorg. Chem.* **1994**, *33*, 403−404. (e) Larsen, S. K.; Pierpont, C. G.; DeMunno, G.; Dolcetti, G. *Inorg. Chem.* **1986**, *25*, 4828−4831. (f) Luo, H. Y.; Liu, S.; Rettig, S. J.; Orvig, C. *Can. J. Chem.* **1995**, *73*, 2272−2281. (g) Baird, D. M.; Fanwick, P. E.; Barwick, T. *Inorg. Chem.* **1985**, *24*, 3753−3758.

Table 1. Crystallographic Data for $[(HCpz_3)Re(OPPh_3)Cl_2]Cl\cdot 0.5CDCl_3$ ([**3**]Cl·0.5$CDCl_3$) and $(HBpz_3)Re(OPPh_3)Cl_2\cdot C_6H_6$ (**4**·C_6H_6)

	[**3**]Cl·0.5 $CDCl_3$	**4**·C_6H_6
empirical formula	$C_{28.5}H_{25}D_{0.5}Cl_{4.5}N_6OPRe$	$C_{33}H_{31}BCl_2N_6OPRe$
fw	845.75	826.52
temp (K)	293	293
λ (Å)	0.710 73 (Mo Kα)	0.710 73 (Mo Kα)
space group	$P\bar{1}$	$P\bar{1}$
total no. of data collected	5511	5890
no. of indep reflns	5511	5890
a (Å)	8.7612(11)	8.867(2)
b (Å)	12.755(2)	11.288(2)
c (Å)	14.418(2)	16.881(3)
α (deg)	81.149(11)	84.22(3)
β (deg)	85.397(9)	85.08(3)
γ (deg)	81.243(12)	89.35(3)
V (Å^3)	1570.8(4)	1674.8(6)
Z	2	2
ρ_{calcd} (g/cm^3)	1.788	1.639
cryst size (mm)	0.45 × 0.25 × 0.05	0.38 × 0.22 × 0.12
μ (mm^{-1})	4.336	3.872
R indices [$I > 4\sigma(I)$][a]	R1 = 0.0301, wR2 = 0.0830	R1 = 0.0180, wR2 = 0.0452
R indices (all data)[a]	R1 = 0.0330, wR2 = 0.0866	R1 = 0.0197, wR2 = 0.0462

[a] $R1 = \sum||F_o| - |F_c||/\sum|F_o|$; $wR2 = (\sum[w(F_o^2 - F_c^2)^2]/\sum w(F_o^2)^2)^{1/2}$.

Table 2. Selected Bond Lengths (Å) and Angles (deg) for $[(HCpz_3)Re(OPPh_3)Cl_2]Cl\cdot 0.5CDCl_3$ ([**3**]Cl·0.5$CDCl_3$) and $(HBpz_3)Re(OPPh_3)Cl_2\cdot C_6H_6$ (**4**·C_6H_6)

	[**3**]Cl·0.5 $CDCl_3$	**4**·C_6H_6		[**3**]Cl·0.5 $CDCl_3$	**4**·C_6H_6
Re−N12	2.063(4)	2.062(2)	Re−Cl1	2.3703(13)	2.3891(11)
Re−N22	2.094(4)	2.084(2)	Re−Cl2	2.3676(13)	2.3824(11)
Re−N32	2.089(4)	2.083(2)	P−O	1.494(4)	1.503(2)
Re−O	2.101(4)	2.103(2)			
N12−Re−N22	83.8(2)	85.02(9)	N32−Re−Cl1	89.04(13)	90.40(7)
N12−Re−N32	84.8(2)	85.16(9)	N12−Re−Cl2	92.59(12)	94.47(7)
N22−Re−N32	85.2(2)	88.34(10)	N22−Re−Cl2	92.01(12)	88.99(7)
N12−Re−O	175.46(14)	173.98(8)	N32−Re−Cl2	176.40(12)	177.33(7)
N22−Re−O	92.3(2)	91.01(9)	O−Re−Cl1	90.44(11)	90.19(6)
N32−Re−O	92.6(2)	90.20(9)	O−Re−Cl2	89.84(12)	89.98(6)
N12−Re−Cl1	93.24(12)	93.68(7)	C11−Re−Cl2	93.60(5)	92.26(4)
N22−Re−Cl1	173.76(11)	178.26(6)	P−O−Re	151.6(2)	149.72(12)

[**1**]Cl, 0.097(3) $M^{-1}\ s^{-1}$ for [**1**]BF_4, and 8.6(6) × $10^{-5}\ M^{-1}\ s^{-1}$ for **2**. Thus, at room temperature, $k_{[1]Cl}/k_2 \approx 550$ and $k_{[1]BF_4}/k_{[1]Cl} \approx 2$.

The reactions of [**1**]Cl and **2** with PPh_3 were also monitored in 1,2-dichlorobenzene. The reduction rate for [**1**]Cl at 25.3 °C is 0.0574(3) $M^{-1}\ s^{-1}$, a 20% increase over the rate in CH_2Cl_2; the rate for **2** is identical to that in dichloromethane. The variation of the rate of reduction of $[\mathbf{1}]^+$ with solvent and counterion suggests that ion-pairing effects have a modest influence on the reaction.

Rate constants were measured over a >30 °C temperature range in 1,2-dichlorobenzene to obtain activation parameters for the two reactions (Table S1a and Figure S4a, Supporting Information). Reduction of [**1**]Cl takes place with $\Delta H^{\ddagger} = 13.4 \pm 0.5$ kcal/mol and $\Delta S^{\ddagger} = -19 \pm 2$ cal·$mol^{-1}\ K^{-1}$ (289−322 K), while **2** is reduced with $\Delta H^{\ddagger} = 17.11 \pm 0.13$ kcal/mol and $\Delta S^{\ddagger} = -19.7 \pm 0.4$ cal·$mol^{-1}\ K^{-1}$ (291−351 K). The observed entropies of activation are identical within experimental error and are consistent with an associative process. The enhanced rate of reaction of triphenylphosphine with cationic [**1**]Cl is due entirely to a lower enthalpy of activation.

To determine whether oxygen atom transfer is reversible, the phosphine oxide adducts [**3**]Cl and [**4**] were each treated with an excess of $P(C_6D_5)_3$ in CD_2Cl_2. Monitoring by ^{31}P and ^1H NMR spectroscopy revealed no free $P(C_6H_5)_3$ in either case; the only products observed were the $Re^{III}-P(C_6D_5)_3$ adducts and free $OP(C_6H_5)_3$. Thus, the degenerate exchange reaction (eq 4) does not take place at a rate competitive with phosphine oxide dissociation; oxygen atom transfer is effectively irreversible.

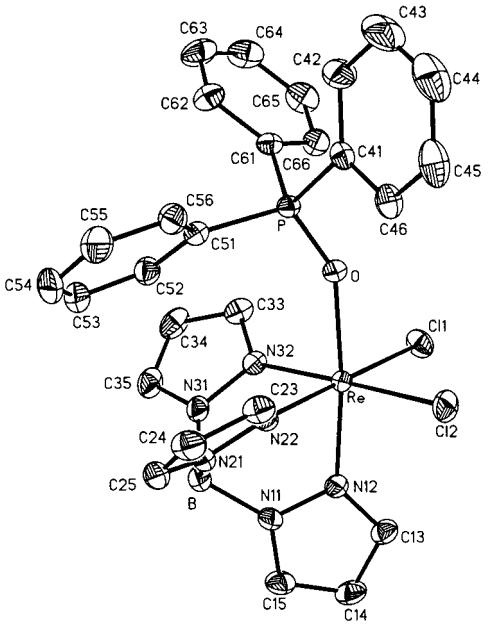

Figure 2. SHELXTL plot (30% thermal ellipsoids) of $(HBpz_3)ReCl_2(OPPh_3)\cdot C_6H_6$ (**4**·C_6H_6). Hydrogen atoms and the solvent of crystallization are omitted for clarity.

Table 3. Second-Order Rate Constants for the Addition of Tertiary Phosphines to [**1**]Cl and **2** (1,2-Dichlorobenzene, 312 K)

PAr_3	$3\sigma_p$[31]	$k_{[1]Cl}$ (M^{-1} s^{-1})	k_2 (M^{-1} s^{-1})
$P(p\text{-}C_6H_4OMe)_3$	−0.81	1.18(6)	$9.27(9) \times 10^{-4}$
$P(p\text{-}C_6H_4Me)_3$	−0.51	0.78(4)	$9.17(7) \times 10^{-4}$
$P(C_6H_5)_3$	0.00	0.181(3)	$3.58(3) \times 10^{-4}$
$P(p\text{-}C_6H_4Cl)_3$	+0.69	0.032(3)	$2.08(10) \times 10^{-4}$

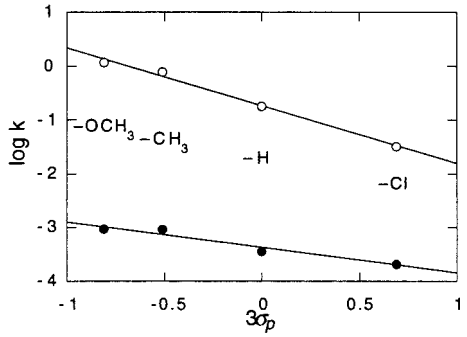

Figure 3. Substituent effects on oxygen atom transfer to $P(p\text{-}C_6H_4X)_3$ from [**1**]Cl (open circles) and **2** (solid circles) in CH_2Cl_2 at 39 °C in $1,2\text{-}C_6H_4Cl_2$. Three times the Hammett σ parameter is used as the ordinate to account for the trisubstitution of the phosphines.

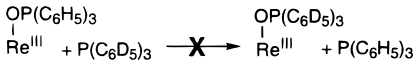

(4)

The reductions of [**1**]Cl and **2** were conducted with several para-substituted triarylphosphines $P(p\text{-}C_6H_4X)_3$ (X = H, Cl, Me, OMe) to explore the effect of phosphine nucleophilicity on reactivity (Table 3). A plot of the logarithms of the rates as a function of the Hammett substituent parameters (σ values)[31] for [**1**]Cl and **2** is shown in Figure 3. A linear correlation is observed in both cases, and the correlation is better with σ ($R^2 = 0.996$ for [**1**]Cl and 0.97 for **2**) than with σ^+ ($R^2 = 0.88$ for [**1**]Cl and 0.87 for **2**). The rates of reaction increase as phosphine nucleophilicity increases for both rhenium complexes, but the cationic complex $[\mathbf{1}]^+$ is more sensitive to this electronic effect ($\rho_{[1]+} = -1.08$; $\rho_2 = -0.47$).

Ligand Substitution Kinetics. The phosphine oxide adducts [**3**]BF_4 and **4** undergo clean ligand substitution when treated with pyridine in chlorinated solvents to give the corresponding pyridine adducts $[(HCpz_3)ReCl_2(py)]BF_4$ and $(HBpz_3)ReCl_2(py)$,[29] respectively. Ligand substitution reactions carried out with [**3**]Cl and pyridine at elevated temperatures also produce $[(HCpz_3)ReCl_2(py)]^+$ at rates similar to those of the tetrafluoroborate salt. However, reactions of the chloride salt are not amenable to detailed kinetic study due to formation of an insoluble byproduct, possibly $(HCpz_3)ReCl_3$. Ligand substitution is not significantly accelerated by irradiation ($\lambda = 350$ nm, **4** in CD_3CN).

The kinetics of these ligand substitution reactions were studied spectrophotometrically in 1,2-dichlorobenzene (3% CH_2Cl_2/dichlorobenzene was used for [**3**]BF_4 due to its limited solubility in pure dichlorobenzene). The observed decay is first-order in rhenium. There is no dependence of the rate on pyridine concentration for either complex (Figure S3a,b, Supporting Information), consistent with a dissociative mechanism for ligand substitution. This conclusion is supported by the large positive entropies of activation of the reactions (Table S1b, Figure S4b, Supporting Information): for [**3**]BF_4, $\Delta H^\ddagger = 29.6 \pm 0.5$ kcal/mol and $\Delta S^\ddagger = +10 \pm 2$ cal·mol^{-1} K^{-1} (324−353 K); for **4**, $\Delta H^\ddagger = 28.4 \pm 0.9$ kcal/mol and $\Delta S^\ddagger = +14 \pm 3$ cal·mol^{-1} K^{-1} (306−337 K). The neutral complex **4** dissociates phosphine oxide about 56 times more rapidly than does cationic $[\mathbf{3}]^+$ ($k_{[3]BF_4} = 4.99(9) \times 10^{-5}$ s^{-1} at 62 °C, $k_4 = 2.80(6) \times 10^{-3}$ s^{-1} at 64 °C).

Discussion

Tris(pyrazolyl)borate and Tris(pyrazolyl)methane as Homologous Ligands. To discern the effect of charge on oxygen atom transfer, we set out to prepare the tris(pyrazolyl)methane rhenium(V) oxo complex $[(HCpz_3)ReOCl_2]^+$ ($[\mathbf{1}]^+$) as a cationic analogue of the known[11−13] neutral tris(pyrazolyl)borate complex $(HBpz_3)ReOCl_2$ (**2**). It was hoped that this minimal perturbation—substitution of a carbon for a boron remote from the metal—would allow a change in charge without significant changes in other steric or electronic properties. The suitability of this comparison was in some doubt because the two ligands are known to differ in binding strength. Reger has reported in his work with lead(II) and tin(II) that neutral tris(pyrazolyl)methane ligands do not bind as tightly as the anionic tris(pyrazolyl)borate analogues.[32] Vahrenkamp has noted similar behavior in his studies of zinc(II) coordination compounds possessing tripodal ligands: whereas tris(pyrazolyl)borate ligands are reliably tridentate, the tris(pyrazolyl)methane analogues are often bidentate.[33] The lability of the tris(3,5-dimethylpyrazolyl)methane ligand in oxomolybdenum(V) complexes complicates their isolation.[34] The difference in binding strength is also evident in oxorhenium complexes. Herrmann has reported that $[(HCpz_3)ReO_3]^+$ is rather sensitive to hydrolysis,[18] in contrast to the marked stability of $(HBpz_3)ReO_3$.[35] Likewise, $[(HCpz_3)ReOCl_2]Cl$ ([**1**]Cl) slowly dissociates $HCpz_3$ in acetonitrile at room temperature, where $(HBpz_3)ReOCl_2$ (**2**) is stable indefinitely.

In contrast to the differences in binding affinity, $HCpz_3$ and $HBpz_3^-$ do appear to confer very similar properties on the static structures of their metal complexes. The spectral data presented here establish that the rhenium(V) complexes $[(HCpz_3)ReOCl_2]^+$ ($[\mathbf{1}]^+$) and $(HBpz_3)ReOCl_2$ (**2**) are close analogues. The ^1H NMR data for both complexes show diamagnetic species possessing tridentate poly(pyrazolyl) ligands with mirror symmetry. The rhenium-oxo stretches in the IR spectra are nearly identical ($\nu_{[1]Cl} = 987$ cm^{-1}, $\nu_2 = 975$ cm^{-1}), as are the λ_{max} and ϵ values in the UV−vis spectra (for [**1**]Cl $\lambda_{max} = 678$ nm, $\epsilon = 120$ M^{-1} cm^{-1}; for **2**, $\lambda_{max} = 690$ nm, $\epsilon = 125$ M^{-1} cm^{-1}).

Unfortunately, positional disorder involving the oxo and chlorine ligands[24] precluded obtaining reasonable metrical data for [**1**]Cl[23] and **2**.[25] X-ray crystallographic data for the rhenium(III) phosphine oxide adducts $[(HCpz_3)ReCl_2(OPPh_3)]$-Cl ([**3**]Cl) and $(HBpz_3)ReCl_2(OPPh_3)$ (**4**) show that these two metal complexes have qualitatively identical structures (Figures 1 and 2). Even quantitative differences in bond lengths and angles are remarkably small (Table 2). The only statistically significant difference in bond lengths are in the Re−Cl bond distances, and even here the differences are less than 0.02 Å. These results are in line with other structural comparisons in

(31) Hansch, C.; Leo, A.; Taft, R. W. *Chem. Rev.* **1991**, *91*, 165−195.

(32) (a) Reger, D. L.; Collins, J. E.; Rheingold, A. L.; Liable-Sands, L. M. *Inorg. Chem.* **1999**, *38*, 3235−3237. (b) Reger, D. L.; Collins, J. E.; Rheingold, A. L.; Liable-Sands, L. M.; Yap, G. P. A. *Inorg. Chem.* **1997**, *36*, 345−351. (c) Reger, D. L.; Collins, J. E.; Myers, S. M.; Rheingold, A. L.; Liable-Sands, L. M. *Inorg. Chem.* **1996**, *35*, 4904−4909.

(33) Titze, C.; Hermann, J.; Vahrenkamp, H. *Chem. Ber.* **1995**, *128*, 1095−1103.

(34) Dhawan, I. K.; Bruck, M. A.; Schilling, B.; Grittini, C.; Enemark, J. H. *Inorg. Chem.* **1995**, *34*, 3801−3808.

(35) Degnan, I. A.; Herrmann, W. A.; Herdtweck, E. *Chem. Ber.* **1990**, *123*, 1347−1349.

the literature, which show that complexes of tris(pyrazolyl)-borates and tris(pyrazolyl)methanes can have essentially identical structures.[32−33,36−37] We conclude that the rhenium(V) oxo compounds [**1**]$^+$ and **2** are isosteric and isoelectronic analogues, as are the phosphine oxide adducts [**3**]$^+$ and **4**. Thus, differences in reactivity may be attributed primarily to the difference in overall charge.

Charge Effects on Atom Transfer. Most metal oxo complexes oxidize triphenylphosphine to triphenylphosphine oxide.[5] The mechanism has been discussed extensively, and is generally believed to involve direct attack of the phosphine at the oxo ligand.[7,38−39] The reactions described here also appear to follow this mechanism. The kinetics are cleanly bimolecular, and substituent effects on the phosphine are consistent with nucleophilic attack by the phosphine at oxygen. Initial outer-sphere electron transfer appears unlikely, given the low propensity of rhenium(V) oxo complexes to act as outer-sphere oxidants.[40] Prior coordination of the phosphine to the metal center[41] also seems improbable given the coordinative saturation of these octahedral complexes. Note that dissociation of the $HCpz_3$ ligand is not observed in the noncoordinating solvents in which oxygen atom transfer has been studied, and even in acetonitrile takes place much more slowly than reaction with phosphine.

Compounds possessing the $[Re{\equiv}O]^{3+}$ core exhibit a wide range of reactivity toward PPh_3. At one end of the spectrum are complexes which show no reactivity at the oxygen atom. $(HBpz_3)ReO(Ph)Cl$, for example, does not react with phosphine,[29] and the dimeric oxorhenium(V) chelate $[CH_3ReO(LS_2)]_2$ ligates PPh_3 to form 2 equiv of monomeric $CH_3ReO(LS_2)(PPh_3)$ without undergoing reduction (LS_2 = *o*-$SC_6H_4CH_2S$).[42] Many rhenium(V) oxo compounds are reduced by PPh_3 to form deoxygenated products. $[ReO(SPh)_4^-]$[43] and $(Ph_3P)_2ReOCl_3$[44] are typical examples, reacting with PPh_3 in refluxing acetonitrile to form rhenium(III) phosphine adducts. At the reactive end of the spectrum is the cationic $[(Me_3tacn)ReOCl_2]^+$ (Me_3tacn = 1,4,7-trimethyl-1,4,7-triazacyclononane), which is reduced within a day at room temperature.[38]

While the reduction of **2** is typical, requiring elevated temperatures or prolonged times, the reaction of [**1**]$^+$ with triphenylphosphine is as fast as any reported for a rhenium(V) oxo complex. Despite having nearly identical ligand environments, the cationic complex [**1**]BF_4 reacts about *1000 times faster* than the neutral tris(pyrazolyl)borate compound **2** in dichloromethane at room temperature. This dramatic rate enhancement is the first clean and quantitative example of a charge effect on oxygen atom transfer and shows that this effect can rival or eclipse typical effects exerted by changing ligand environments.[45]

A key question is whether the charge effect on atom transfer is primarily kinetic or thermodynamic in origin. One could argue that the cation reacts faster because there is a greater driving force for atom transfer, either because the cation has an intrinsically weaker Re≡O bond or because the cationic fragment binds the phosphine oxide more tightly. While we cannot rule out the former effect, it seems unlikely to be large, given the body of evidence in the organic literature suggesting that polar effects on bond strength are minimal.[46] The effects of charge on ligand binding can be addressed using the results of the study of ligand substitution reactions of the phosphine oxide adducts [**3**]$^+$ and **4**. Since these reactions are dissociative, the energies of activation for ligand loss are approximately equal to the equilibrium binding energies of the ligands. Cationic [**3**]$^+$ does indeed bind phosphine oxide more tightly than neutral **4**, as indicated by its slower rate of ligand dissociation. However, the quantitative difference in binding ($\Delta\Delta H^{\ddagger}_{diss}$ = 1.2 kcal/mol) is much smaller than the kinetic difference in oxygen atom transfer ($\Delta\Delta H^{\ddagger}_{redn}$ = 3.7 kcal/mol). Thus, while tighter binding of phosphine oxide may contribute to the rate difference, it cannot be its major determinant.

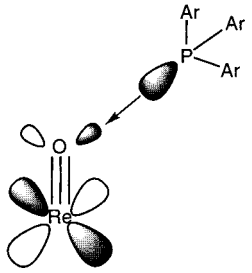

Figure 4. Orbital interactions in oxygen atom transfer.

The observed substituent effects on atom transfer also indicate that thermodynamic effects exert a relatively minor influence on the reaction rate. The reductions of both $[(HCpz_3)ReOCl_2]^+$ ([**1**]$^+$) and $(HBpz_3)ReOCl_2$ (**2**) go faster as the triarylphosphines become more electron-rich (Table 3). Qualitatively, both reactions involve nucleophilic attack of the phosphine at the oxo group. Quantitatively, though, there is again a significant difference: cationic [**1**]$^+$ is much more sensitive to changes in phosphine substituent than **2** (Figure 3; $\rho_{[1]^+}$ = −1.08; ρ_2 = −0.47). One would expect the opposite if reduction of [**1**]$^+$ were favored by substantial driving force effects, for by the Hammond postulate the more exothermic reaction should be the *less* selective. The greater selectivity of [**1**]$^+$ points to a kinetic effect, with the positive charge influencing the stability of the transition state. This result is in line with other studies of atom transfer that find poor correlations of reaction kinetics with thermodynamic driving force.[47]

The charge effect can be rationalized by considering the molecular orbitals involved in the reaction. Increasing the overall charge on the metal complex should lower the energy of all the molecular orbitals, in particular the M≡O π^* orbital which interacts with the phosphorus lone pair in the transition state for reduction (Figure 4). The metal LUMO−phosphine HOMO interaction will therefore be stronger for the cationic complex, and the reduction will go faster. In other words, the cationic species is more electrophilic than the neutral, a result which

(36) Bhambri, S.; Tocher, D. A. *Polyhedron* **1996**, *15*, 2763−2770.
(37) Humphrey, E. R.; Mann, K. L. V.; Reeves, Z. R.; Behrendt, A.; Jeffery, J. C.; Maher, J. P.; McCleverty, J. A.; Ward, M. D. *New J. Chem.* **1999**, *23*, 417−423.
(38) Conry, R. R.; Mayer, J. M. *Inorg. Chem.* **1990**, *29*, 4862−4867.
(39) Pietsch, M. A.; Hall, M. B. *Inorg. Chem.* **1996**, *35*, 1273−1278.
(40) Böhm, G.; Wieghardt, K.; Nuber, B.; Weiss, J. *Inorg. Chem.* **1991**, *30*, 3464−3476.
(41) This possibility has been conclusively excluded in the reactions of $[(bpy)_2RuO(PR_3)]^{2+}$, where atom transfer is observed to exogenous phosphine in preference to bound phosphine: Marmion, M. E.; Takeuchi, K. J. *J. Am. Chem. Soc.* **1986**, *108*, 510−511.
(42) Jacob, J.; Guzei, I. A.; Espenson, J. H. *Inorg. Chem.* **1999**, *38*, 1040−1041.
(43) Dilworth, J. R.; Neaves, B. D.; Hutchinson, J. P.; Zubieta, J. A. *Inorg. Chim. Acta* **1982**, *65*, L223−L224.
(44) Rouschias, G.: Wilkinson, G. *J. Chem. Soc. A* **1967**, 993−1000.
(45) (a) Wong, Y. L.; Ma, J. F.; Law, W. F.; Yan, Y.; Wong, W. T.; Zhang, Z. Y.; Mak, T. C. W.; Ng, D. K. P. *Eur. J. Inorg. Chem.* **1999**, 313−321. (b) Donahue, J. P.; Goldsmith, C. R.; Nadiminti, U.; Holm, R. H. *J. Am. Chem. Soc.* **1998**, *120*, 12869−12881.
(46) (a) Bordwell, F. G.; Zhang, X. M. *J. Am. Chem. Soc.* **1994**, *116*, 973−976. (b) Zhang, X. M.; Bordwell, F. G. *J. Am. Chem. Soc.* **1994**, *116*, 968−972.
(47) Abu-Omar, M. M.; Appelman, E. H.; Espenson, J. H. *Inorg. Chem.* **1996**, *35*, 7751−7757.

has been suggested in other studies of metal oxo complexes.[48] What is remarkable is the magnitude of the effect revealed by the present study: an increase of one unit of positive charge accelerates atom transfer by 2−3 orders of magnitude.

Conclusions

Spectroscopic comparison of the new rhenium(V) oxo complex $[(HCpz_3)ReOCl_2]^+$ ($[\mathbf{1}]^+$) and the known complex $(HBpz_3)ReOCl_2$ (**2**) and structural comparison of the corresponding phosphine oxide adducts $[(HCpz_3)Re(OPPh_3)Cl_2]^+$ ($[\mathbf{3}]^+$) and $(HBpz_3)Re(OPPh_3)Cl_2$ (**4**) demonstrate that $HBpz_3$ and $HCpz_3$ are isoelectronic and isostructural analogues. The difference in charge creates substantial differences in reaction rates. Oxygen atom transfer is accelerated by a factor of ∼1000 in the cationic complex $[\mathbf{1}]^+$ as compared to neutral **2**. This effect is much larger than the difference in ligand substitution rates (cationic $[\mathbf{3}]^+$ dissociates $OPPh_3$ about 50 times more slowly than neutral **4**) and appears to be primarily a transition-state effect. This large effect suggests that charge may be as important as the nature of ancillary ligands in tuning the reactivity of oxometal species.

Acknowledgment. We thank Dr. Maoyu Shang for his assistance with the X-ray structures. Support from the National Science Foundation (Grant CHE-97-33321-CAREER), the Camille and Henry Dreyfus Foundation (New Professor Award to S.N.B.), DuPont (Young Professor Award to S.N.B.), and the University of Notre Dame are gratefully acknowledged.

Supporting Information Available: Figures and tables of kinetic data for the phosphine reductions of [**1**]Cl and **2** and ligand substitution of pyridine for $OPPh_3$ in [**3**]BF_4 and **4** and tables of crystallographic parameters, atomic coordinates, bond lengths and angles, anisotropic thermal parameters, and hydrogen coordinates for [**3**]Cl·0.5$CDCl_3$ and **4**·C_6H_6. This material is available free of charge via the Internet at http://pubs.acs.org.

IC990851B

(48) (a) DuMez, D. D.; Mayer, J. M. *Inorg. Chem.* **1995**, *34*, 6396−6401. (b) Brown, S. N.; Mayer, J. M. *J. Am. Chem. Soc.* **1996**, *118*, 12119−12133. (c) DuMez, D. D.; Mayer, J. M. *Inorg. Chem.* **1998**, *37*, 445−453.